Proceedings of 2008 ASME Summer Heat Transfer Conference
HT2008
August 10-14, 2008, Jacksonville, Florida USA

HT2008-56349

VIBRATION/SHOCK-TOLERANT CAPILLARY TWO-PHASE LOOP TECHNOLOGY FOR VEHICLE THERMAL CONTROL

Xudong Tang
Advanced Cooling Technologies, Inc.
1046 New Holland Avenue
Lancaster, PA 17601
e-mail: xudong.tang@1-act.com

Chanwoo Park
Mechanical Engineering Department
University of Nevada, Reno, NV 89557

ABSTRACT

Two-phase thermal management technologies are promising cooling solutions for the high performance electronics in the next generation military and commercial vehicles. However, vibrations (~ 10Grms in commercial automobile engines and transmissions) and shocks (30G to 1,200G in military combat vehicles, caused by gun firing, ballistic launch and abrupt maneuvering) present a severe challenge to any capillary-driven (i.e., passive) two-phase devices. A low-cost, vibration/shock-tolerant Capillary Two-Phase Loop (CTPL) technology was developed as a cooling alternative for the future military vehicles. Unlike the traditional two-phase cooling loops such as Loop Heat Pipes (LHP) and Capillary Pumped Loops (CPL), the CTPL offers the following advantages: (1) lower manufacturing cost by sintering the evaporator wick in-situ; (2) improved tolerance to vibrations and shocks due to the improved mechanical strengths of the in-situ sintered wick; (3) improved heat flux performance because of the non-inverted meniscus wick. Small-scale proof-to-concept CTPL prototypes were successfully tested up to 120W of heat input and under multiple, consecutive shocks of up to 6.6G.

INTRODUCTION

It is becoming increasingly common to mount the vehicle powertrain electronics directly onto the internal combustion engines and transmissions instead of the traditional locations inside the passenger compartment. The new packaging trend aims to shorten the connection wires between the electronic components and the control objects, accomplishing more compact and cost-effective packaging with greater design flexibility. However, this approach could introduce vibration-induced issues to the powertrain electronics, which eventually could deteriorate the structural and cooling performance of the electronics.

From the data available [1], the vibration conditions in commercial automobiles ranges from 10 Grms (root-mean-square of acceleration) on the engine and transmission to 3~5 Grms in the passenger compartment. Power Spectral Density (PSD) at a particular location over certain frequency bands is typically used for quantitative analysis of the random vibrations in the vehicles. Unlike commercial vehicles, military combat vehicles could have additional shock sources from gun firing, ballistic launch and abrupt maneuvering. The mechanical shock environment in combat vehicles is classified as Basic, Gun Firing, Operational Ballistic or High Intensity. A "Basic" shock can be at 30 G in an 11 ms half-sine wave, while a "High Intensity" shock can be 1,200 G in a 1 ms half-sine wave.

Two-phase thermal management technologies are promising cooling solutions for the electronics in the next generation military vehicles. Loop Heat Pipes (LHP) [2-4] and Capillary Pumped Loops (CPL) [5-7] are capable of transporting large heat loads over long distances as required by many military vehicles. Besides the terrestrial applications, LHPs and CPLs have also been increasingly used for spacecraft thermal control due to their passive operation and high reliability.

The shocks and vibrations in a military combat vehicle present a severe challenge to these passive

capillary-driven devices. Resonant vibrations could break the liquid-vapor meniscus in the evaporator wick, potentially resulting in fatal impacts on the performance of the capillary devices. Mechanical shocks may disturb the fluid distribution in the hydraulic lines of the two-phase loop, which greatly affects the start up behaviors and long-term operating characteristics. Excessive mechanical shocks could even damage the internal structure of the evaporator such as the knife-edge seal in LHP. In addition to the shock and vibration issues, LHPs and CPLs require precision machining and insertion of fine pore wicks. This is a significant cost driver and inhibitor for high volume application of such devices.

In the work presented in this paper, we developed a small-scale low-cost, vibration/shock tolerant Capillary Two-Phase Loop (CTPL) technology. This investigation is intended to gain fundamental knowledge on the overall operational characteristics and design aspects of CTPLs. The effects related to the variations on heat load applied and its capability to maintain a steady operation under shock conditions were investigated.

NOMENCLATURE

A_{wick}	wick cross-sectional area (m^2)
D	transportation line diameter (m)
f	frication factor
K_{wick}	wick permeability (m^2)
L	transportation line length (m)
L_{wick}	wick effective length (m)
$\dot{m}$	mass flowrate (kg/s)
P_{cap}	capillary pressure (Pa)
Re	Reynolds number
r_P	mean pore radius (m)
ρ	density (kg/m^3)
σ	surface tension (N/m)
ΔP_{liquid}	liquid line pressure drop (Pa)
ΔP_{vapor}	vapor line pressure drop (Pa)
ΔP_{wick}	porous wick pressure drop (Pa)
μ	liquid dynamic viscosity (Pa s)

1. WORKING PRINCIPLE

Figure 1 illustrates the concept of the proposed CTPL technology. The proof-of-concept CTPL is basically composed of the following components: a capillary evaporator (responsible for generating capillary forces that drive the working fluid), a condenser, a liquid reservoir (to ensure a healthy system startup), liquid and vapor lines.

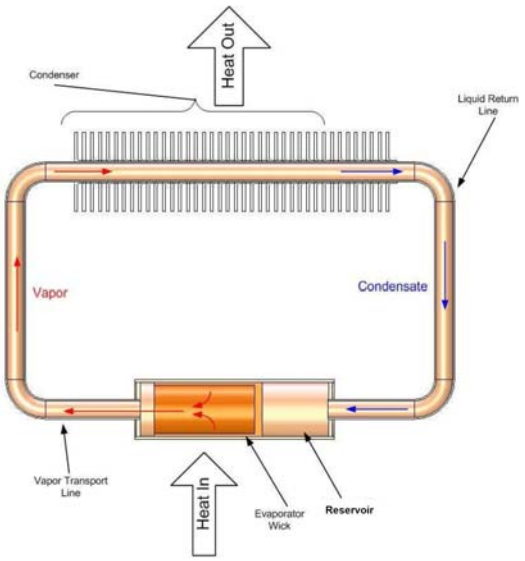

Figure 1. Concept of capillary two-phase loop

The capillary forces are generated by the capillary evaporator, which acquires heat and transfers it to the working fluid. Latent heat is transferred to the working fluid starting the evaporation process. A meniscus is formed at the liquid/vapor interface, which is responsible for developing the capillary pressure that will drive the working fluid from the condenser to the reservoir, and eventually into the evaporator. Vapor is displaced from the evaporator and becomes condensate in the condenser. The CTPL can be used to transfer heat over long distances with small pressure drops over the entire loop allowing its use in large systems.

There are two major ways that vibrations and shocks disturb the operation of the capillary-driven device. First, the impact of the vibrations and shocks on the liquid-vapor meniscus in the evaporator wick can break the capillary membrane and result in the fatal condition of the capillarity. The second disturbance would happen in the reservoir and transport lines that contain large liquid mass. When the liquid mass is subject to a low frequency and high amplitude shock, the liquid displacement could result in long-lasting or permanent interruptions of the liquid supply to the evaporator wick.

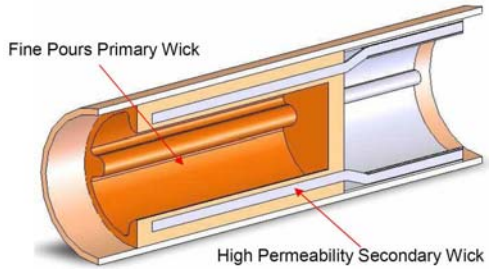

Figure 2. Schematic of capillary evaporator with graded wick structure design

The CTPL differs from the traditional LHPs and CPLs in the evaporator design. As shown in Figure 2, it uses a primary wick with fine-pore barrier layer facing the vapor volume. The fine pores provide stronger capillary action to counter the disturbances caused by the shock and vibration. A secondary wick of high permeability is used to provide quicker liquid replenishment to the primary wick in case of a liquid depletion caused by shocks. The evaporator porous wick structure are sintered in-situ, eliminating the expensive steps of wick machining, insertion and knife-edge sealing as required by the LHPs and CPLs, which also is inherently strong to survive severe shocks and vibrations. The use of graded wicks renders it capable of mitigating the vibration and shock impact on the liquid-vapor interface (meniscus), while providing high heat flux removal capability due to its low thermal resistance and low wick pressure drop.

2. EXPERIMENTAL APPARATUS

2.1 Evaporator Development

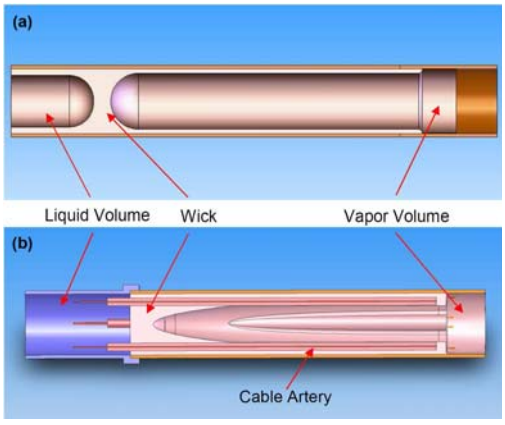

Figure 3. (a) Baseline evaporator; (b) Cable artery evaporator

In the present investigation, two cylindrical evaporator prototypes, a baseline evaporator and a cable artery evaporator, were fabricated and tested in the proof-of-concept CTPL. The specifications can be found in Table 1.

Table 1. Specification of CTPL evaporators

Base Line Evaporator	
Total Length (cm)	12.7
Active Wick Length (cm)	8.6
Tube OD/ID (cm)	1.91 / 1.73
Tube Material	101 Copper
Wick OD/ID (cm)	1.73 / 1.50
Wick Material	-270/325 Copper powder
Capillary Pressure (kPa)	4.83
Permeability (m^2)	2×10^{-12}
Cable Artery Evaporator	
Total Length (cm)	12.7
Active Wick Length (cm)	7.4
Tube OD/ID (cm)	1.91 / 1.73
Tube Material	101 Copper
Wick OD (cm)	1.73
Wick Material	345 Copper powder
Artery Material *	-230/270 copper powder
Artery Length (cm)	10.2
Artery Diameter (cm)	0.25
Capillary Pressure (kPa)	8.27
Permeability (m^2) **	2.5×10^{-12}

* Cables were made of braided copper wires

** Estimated due to the measurement difficulty

The baseline evaporator as shown in Figure 3(a) was constructed to have a concave-shape wick structure inside a copper envelope, which was sintered with fine copper powder. A copper wick wall divided the evaporator into vapor and liquid volume. The heat was introduced through the copper wall and wick layer around the vapor volume. The concave-shape wick structure provided a large evaporation surface and meanwhile a low thermal resistance.

To achieve high capillary pumping pressure while minimizing the pressure drop in the wick, a cable artery evaporator was developed. Figure 3(b) shows the arterial evaporator wick design, which is similar to the baseline evaporator. Firstly, four cable arteries were made out of relatively coarse sintered copper powder and braided copper cables. Then, they were re-sintered with finer copper powder in an oxygen-free copper tube. To avoid the vapor backflow into the liquid volume through cable arteries, the cable arteries were embedded in the main fine copper wick layer without directly contacting with the vapor volume. In the cable artery evaporator design, the main fine copper wick layer provided high capillary pumping pressure, while the highly permeable cable arteries

reduced the flow resistance (or liquid pressure drop) from the liquid to vapor side. Therefore, the heat flux performance of the capillary two-phase loop can be maximized.

2.2 Loop Development

A proof-of-concept CTPL was fabricated and tested to demonstrate the CTPL operation as well as to evaluate the performance of various evaporator designs under shock/vibration conditions. Figure 4 shows the CTPL test setup, which consists of an evaporator, a condenser, transport lines between them, and a reservoir. The transport lines of the CTPL are divided into two sections: one for the vapor and the other for the liquid.

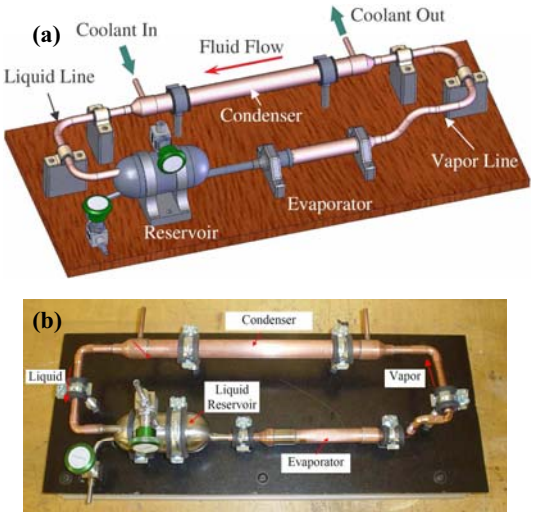

Figure 4. (1) CTPL Solid; (2) CTPL prototype

The investigated CTPL was basically a copper/water system. In the loop illustrated in Figure 4, the vapor/liquid flowed in a counter-clock wise direction. An aluminum heater block with cartridge heats was mounted on the vapor side of the evaporator. Heat was introduced into the evaporator through the heater block. A double tube was used as the condenser. A cylindrical reservoir was installed between the liquid line and the evaporator. The reservoir was mounted on a higher elevation than the evaporator. Therefore, as long as the system was charged with sufficient amount of liquid, and was to test in horizontal condition only (orientation effects were not investigated in this work), this reservoir setup can ensure the liquid supply to the evaporator during start up, normal operation and even the shock condition. A copper tube was used to connect the evaporator and reservoir for the liquid supply. It has a small diameter, which can effectively mitigate or choke the bulky liquid churning motion induced by the vibration or shock. In order to avoid the possibility of the structure damage during the shock test, unnecessary masses (pressure transducer, fittings and etc.) were removed. The height of the loop was also reduced for the shock test. Each component was firmly assembled on a test panel with supporting brackets.

Table 2. Specifications of CTPL

	Condenser	*Reservoir*
Length (cm)	27.9	11.7
OD/ID (cm)	0.97 / 0.79	5.08 / 4.62
Volume (cc)	13.6	169
	Vapor Line	*Liquid Line*
Length (cm)	35.8	24.1
OD/ID (cm)	0.97 / 0.79	0.97 / 0.79
Volume (cc)	17.4	11.8

The specifications of the CTPL are listed in Table 2. The working fluid (water) in CTPL must operate without impurities to avoid the presence of non-condensable gases in the loop. Prior to charging the CTPL with water, the loop was leak-checked using a helium mass spectrometer. A vacuum of at least 1×10^{-5} Torr had to be accomplished and sustained by the experimental apparatus. to ensuring a good vacuum condition. Then a total of 190 cc distilled water was charged into the system using standard two-phase system processing procedures to minimize contaminants and the presence of non-condensable gases.

The CPTL design is essentially about to balance the maximum capillary pressure and pressure drop in the loop. Capillary pressure is developed by the wick structure and working fluid, which can be can be calculated using the Young–Laplace equation:

$$P_{cap} = \frac{2\sigma}{r_p} \tag{1}$$

The overall pressure drop in the loop must be less than the maximum capillary pressure in order to ensure that the system will operate continuously.

$$P_{cap} \geq \Delta P_{wick} + \Delta P_{vapor} + \Delta P_{liquid} \tag{2}$$

The major components of the CTPL pressure drop are related to the flow in the wick structure, vapor and the liquid lines. The pressure drop in the porous wick structure was calculated by Darcy's Law.

$$\Delta P_{wick} = \frac{\mu L_{wick}\dot{m}}{\rho K_{wick} A_{wick}} \tag{3}$$

For either vapor or liquid lines, the pressure drop can be calculated using the following equation

$$\Delta P = f(\mathrm{Re})\rho\frac{v^2 l}{2D} \tag{4}$$

where l is the length of either liquid or vapor line, and $f(\mathrm{Re})$ is dependent on the Reynolds number of each phase. The friction factor can be determined by

$$f = \begin{cases} \dfrac{64}{\mathrm{Re}} & (\mathrm{Re} < 2{,}200) \\ 0.00063\sqrt{\mathrm{Re}} & (2{,}220 \le \mathrm{Re} < 4{,}000) \\ 0.316\,\mathrm{Re}^{-0.25} & (4{,}000 \le \mathrm{Re} < 100{,}000) \\ 0.0032 + 0.22\,\mathrm{Re}^{-0.237} & (\mathrm{Re} \ge 100{,}000) \end{cases} \tag{5}$$

The working fluid mass flowrate in the CTPL under steady state operation can be calculated by

$$\dot{m} = \frac{Q}{c(T_H - T_L) + L} \tag{6}$$

Where c and L are the water specific heat and latent heat, respectively. T_H is the boiling temperature in the evaporator, and T_L is the heat sink (coolant) temperature.

Based on the capillary pressure and permeability provided in Table 1, the CTPL with the base line evaporator design was predicted to be able to remove 70 W heat from the heat source. Although the CTPL with the cable artery design had less capillary pressure, it was predicted to be able to dissipate 150 W heat from the heat source, because it had a high permeability wick structure and therefore less pressure drop in the system. In the calculations above, 50°C condenser temperature was used to simulate the worst case scenario of terrestrial applications.

2.3 Shock Table Development

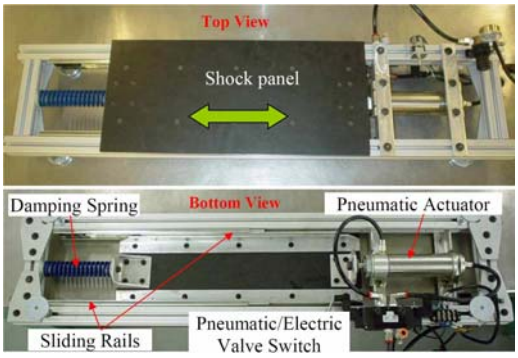

Figure 5. Pneumatically-driven shock table

In order to operate the CTPL under the shock condition, a pneumatically-driven shock table was built (shown in Figure 5). The shock panel was mounted on the sliding rails of a stationary 80/20 aluminum frame. A pneumatic actuator was used to provide the shock force to shock panel. The charging and releasing of the compressed air in the actuator was controlled by a 3-way solenoid valve, a pressure regulator and an electric switch.

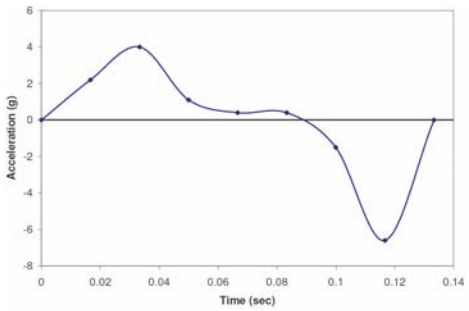

Figure 6. Shock profile of pneumatic shock table

The relative motion of the shock panel against the stationary frame was visually measured using a digital camcorder, which was capable of recording video at a rate of 60 frames per second. The instantaneous displacement of the shock panel was identified in each frame. The acceleration (shock profile) can then be analyzed. The motion of the shock panel from one end to the other lasted for about 0.12 seconds. The calculated instantaneous acceleration is shown in Figure 6. The maximum acceleration was estimated to be 4g and the maximum deceleration was estimated to be 6.6g.

3. RESULTS AND DISCUSSIONS

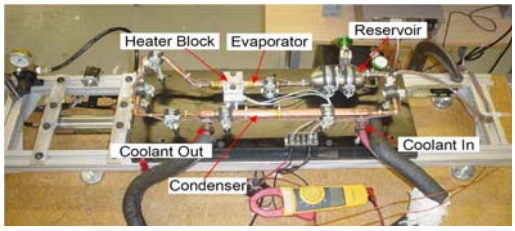

Figure 7. CTPL assembled with shock table

The CTPL was assembled on the shock table, as shown in Figure 7. An Ethylene Glycol chiller was used to provide constant temperature (50°C) coolant to the condenser. The whole loop was well insulated for the purpose of accurate calorimetric study. Type-T thermocouples were used to measure the temperature of evaporator body, vapor line, coolant, liquid line and reservoir.

The profile tests were carried out in order to verify the CTPL behavior for different heat loads applied to the capillary evaporator. The baseline evaporator and the cable artery evaporator were tested in the CTPL

respectively. The stationary condition was tested first. Then the shock condition was introduced.

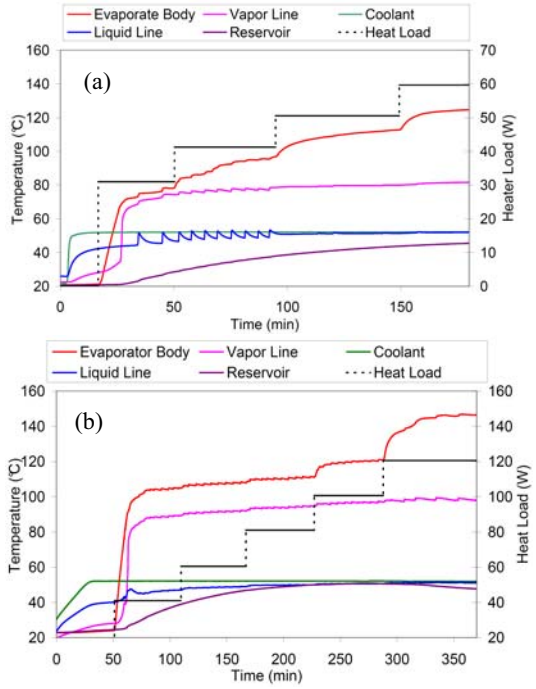

Figure 8. CTPL temperature profile Vs heat load under stationary condition: (a) baseline evaporator; (b) cable artery evaporator

Figure 8 presented the CTPL performance test results under the stationary condition. The CTPL with the baseline evaporator was tested up 60 W (see Figure 8(a)) heat load. The vapor temperature remained at around 80°C. The CTPL with the cable artery evaporator was tested up 120 W with a maximum heat flux of 16 W/cm^2 (see Figure 8(b)). The vapor temperature remained at around 90°C. The cable artery evaporator design was proved to have better performance, because the high permeability arteries embedded in the wick structure reduced the flow pressure drop and thus increased the high heat flux capability. It can be seen that the evaporator maximum performance in tests, 60W for baseline evaporator and 120W for the cable artery evaporator, agreed well with the modeling results in the previous section. The discrepancy could be explained as: (1) the model cannot accurately capture the pressure drop and temperature distribution in the evaporator due to its 2-D geometry wick structure; (2) the permeability of the cable artery evaporator was not accurate.

It can be observed that when the heat load was introduced, the CTPL showed very fast response with very short transients until reaching the steady state. When the heat load was changed, the capillary evaporator did not exhibit any temperature overshoot while entire system was seeking another equilibrium status. The quick startup and stable operation temperature characteristics indicated the CTPL presented a very robust design.

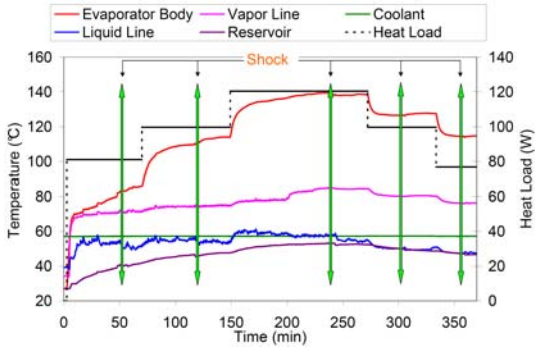

Figure 9. CTPL temperature profile Vs heat load under shock condition

After the stationary test, the shock condition was applied to the CTPL with the artery. At each given heat load, when the CTPL reached the steady state operation, multiple consecutive shocks were then introduced. The shock condition lasted one (1) minute, including four (4) individual shocks. Each shock shared the same shock profile as shown in Figure 6. The test results of temperature profile in Figure 9 indicated that the shock condition did not create significant temperature fluctuation or spike in the CTPL. It was showed that the maximum capacity for the CTPL with the cable artery evaporator was 120 W at a vapor temperature of 83°C, similar to the stationary results. It can be concluded that the CTPL as well as the sintered wick structure were strong enough to survive from this shock condition. Furthermore, the graded wick structure in the cable artery evaporator was proven to be able to maintain the integrity of liquid-vapor meniscus, and avoid the fatal condition of capillarity induced by shocks.

CONCLUSIONS

Small-scale proof-to-concept capillary two-phase loop was developed. Two different capillary evaporator: baseline and cable artery design, were fabricated. Thermal tests were performed to evaluate its performance when different heat loads and severe shocks were applied. The tests showed that capillary two-phase loops are efficient heat transfer devices capable of transferring considerable heat flows for distances. From what has been observed from the tests, the CTPL presented good thermal behavior during startup, normal operation and under shock conditions.

The followings are some of the highlights of the CTPL technology:

(1) Low cost in-situ wick sintering was utilized to develop cable artery evaporator in the CTPL.

(2) The evaporator wicks of the CTPL using a non-inverted meniscus design allow it to dissipate high heat fluxes. The cable artery evaporator built in this work was tested up to a heat input of about 120W.

(3) The capability of the CTPL to re-establish its operationability under vibration and shocks was checked. The sintered wick structure was mechanically stronger to survive severe shocks and vibrations. The CTPL was tested using variable heat inputs under multiple shocks up to 6.6G, and remained reliable thermal behavior.

Further investigation will be performed on the evaporator performance responses for various shock orientations, periodic or random vibration for a long period of time, and startup during vibration or shock exposure.

ACKNOWLEDGEMENTS

This work was supported by SBIR Phase I contract (#W56HZV-07-C-0051) from the U.S. Army RDECOM-TARDEC.

REFERENCES

1. Http://www.hamiltonsundstrand.com/

2. Yu.F. Maydanik, 2003, “Loop Heat Pipes”, Applied Thermal Engineering, 25, 635-657

3. R. J. McGlen, R. Jachuck, S. Lin, 2004, “Integrated thermal management techniques for high power electronic devices”, Applied Thermal Engineering , 24, 1143-1156

4. V.G. Pastukhov , Yu.F. Maidanik, 2003, “Miniature loop heat pipes for electronics cooling”, Applied Thermal Engineering, 23, 1125-1135

5. E. Bazzo, R.R. Riehl, 2003, “Operation characteristics of a small-scale capillary”, Applied Thermal Engineering, 23, 687-705

6. J. Ku, 1993, “Overview of capillary pumped loop technology”, ASME HTD Heat Pipes and Capillary Pumped Loops, 236, 1-17

7. J. Yu, H. Chen, 2007, “An experimental investigation on capillary pumped loop with the meshes wick”, International Journal of Heat and Mass Transfer, 50, 4503-4507